Superseding Mal-Operation of Distance Relay Under Stressed System Conditions

Nilesh Kumar Rajalwal and Debomita Ghosh

Abstract Mal-operation of distance relay imposes serious threats to system stability and a big reason for large scale blackouts. These relays operate in its third zone due to the inability of detecting fault during stressed system conditions. These stressed conditions are load encroachment, power swing, voltage instability conditions, extreme contingencies, etc. Conventional distance relay operates on the basis of local measurements. It calculates the impedance from the relay to the fault point for its operation. Load encroachment and power swing are very similar to the symmetrical fault condition and it is difficult for these conventional relays to distinguish these stressed conditions from symmetrical faults. It is therefore important to make the distance relay intelligent enough so that it will be able to discriminate between a fault and stressed system condition. With the advancement in synchro-phasor technology, the drawbacks of conventional relays have been overcome. The wide-area monitoring system (WAMS) is capable of development of online intelligent techniques that can segregate the stressed system condition from any fault. With these advanced techniques, the mal-operation of distance relays can be avoided and thus wide-area blackouts can be stopped. In this chapter, a new scheme for detecting the zone-III operation of distance relay is proposed to discriminate the stressed system conditions such as voltage instability, power swing, or load encroachment from fault. The proposed scheme is based on the monitoring of active and reactive power of the load buses using WAMS. Various cases are created on WSCC-9, IEEE-14 and IEEE-30 bus system to test the performance of the proposed algorithm. The simulations have been done on the MATLAB Simulink platform. Results shows that the proposed method is helpful to avoid the unwanted distance relay operation under stressed system conditions.

Keywords Wide-area monitoring system · Phasor measurement units · Distance relays · Power system protection

N. K. Rajalwal (✉) · D. Ghosh
Department of Electrical and Electronics Engineering, Birla Institute of Technology, Mesra, Ranchi, India
e-mail: nileshrajalwal@bitmesra.ac.in

© The Editor(s) (if applicable) and The Author(s), under exclusive license to Springer Nature Switzerland AG 2021

H. Haes Alhelou et al. (eds.), *Wide Area Power Systems Stability, Protection, and Security*, Power Systems, https://doi.org/10.1007/978-3-030-54275-7_15

Abbreviations

WAMS	Wide-area monitoring system
PMU	Phasor measurement unit
OOS	Out of step
NERC	North American electric reliability corporation
SVM	Support vector machine

Symbols

Z_{seen}	Impedance seen by the relay
P_{iload}	Active power consumption of load bus i
Z_{set}	Impedance setting of distance relay
Q_{iload}	Reactive power consumption of load bus i
Z_{k}	Impedance of element k
P_{set}	Active power setting for distance relay
V_{i}	Voltage phasor of bus i
Q_{set}	Reactive power setting for distance relay
I_{i}	Current phasor of bus i
P_{AB}	Active power flow between bus A and B
δ_i	Phase angle of bus i
Q_{AB}	Reactive power flow between bus A and B

1 Introduction

The unwanted operation of the distance relay in its third zone due to stressed system conditions such as load encroachment, voltage instability or power swing enhances the chances of cascaded system outage of the power system. The traditional distance protection calculates the impedance at relay location on fundamental frequency based on the local information. The measured local impedance reduces in faulty condition and the distance relay operates. Apart from the fault conditions, a stressed system condition may also reduce the measured impedance and the conventional distance relay may mal-operate in its zone-III.

Many researchers have suggested different methods to avoid this unwanted distance relay operation. In some literature, the discrimination between stressed system conditions and a faulty condition is done using the local measurements. In [1], blinders are utilized to avoid the unwanted operation of distance relay during power swing. In [2], a cross blocking criterion is proposed for blocking of the distance relay during power swing by measuring active and reactive power of the system. Another method that discriminate between fault and power swing is proposed based on the

rate of change of voltage intend of taking only the voltage magnitude [3]. Along with the rate of change of voltage, the rate of change of current is also used to avoid unwanted distance relay operation in [4]. Computational intelligent methods such as support vector machine (SVM) is also used for segregation between the fault and stressed system condition and an adaptive neuro-fuzzy inference system is used for power swing blocking in [5]. In [6], a decision-tree based approach is proposed for fault detection by taking the positive sequence voltage, current and zero sequences current as input. With the advancement in the wide-area monitoring system, advance methods based on the PMUs data is also proposed by the researchers. In [7], a method is proposed for the operation of zone-III of a relay, based on adjacent relays operation in their zone-I and zone-II. Various integrity protection schemes are also proposed for avoiding the unwanted operation of distance relay. In [8], the relay boundary setting is changed online based on the data obtained from WAMS. Additionally, a load rejection scheme is proposed for the formation of integrity protection scheme. A relay security index is proposed in [9] to avoid the unwanted distance relay operation. In the same work a system stability index is also proposed for system instability prediction. Another method proposed in [10] to distinguish the faulty condition from the stressed system condition based on the change in active power and angle difference between load and source. A differential power coefficient is proposed in [11] to determine the difference between the stable and unstable power swing using WAMS. In [12], an online sequential extreme learning machine is proposed for discrimination between voltage instability, power swing, and faulty condition. The proposed method consists of a two stage classifier that utilizes the WAMS for the computation.

Each method discussed above has some limitations. Methods based on the local information may suffer in discriminating the fault condition from the stressed condition when system complexity increase. Computational intelligent methods require large training data sets for the operation. Methods based on Thevenin's equivalent need to compute online Thevenin's impedance that requires fast computing efforts. In this chapter, a method based on the monitoring of real-time active & reactive power of the load is proposed for blocking the operation of distance relay. The active & reactive power flow at loads are significantly different during a fault and stressed system conditions. This significant difference is utilized here for proposing a new algorithm for easy discrimination between a fault and the stressed system condition.

2 Distance Relay Mal-Operation Scenarios

In this section load encroachment, power swing, and voltage instability conditions are described and the effect of these scenarios on distance relay characteristic have been discussed.

Figure 1 shows a two bus system having two sources connected at bus A and B with a transmission line between them having an impedance Z_L. The generator 1 connected to bus A has induced EMF $E_1\angle\delta$ and internal impedance Z_1.

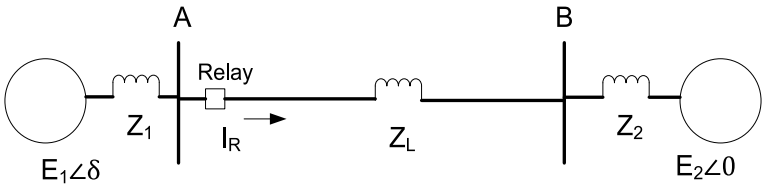

Fig. 1 Two bus system

The generator 2 connected to bus B has an induced EMF of $E_2\angle 0$ and the internal impedance of Z_2. A distance relay is connected in the line near bus A to detect any faulty condition in the transmission line. If V_R and I_R is the voltage and current measured by the relay, then the impedance seen by the relay Z_{seen} will be:

$$Z_{seen} = \frac{V_R}{I_R} \tag{1}$$

A fault in line AB will increase the value of current I_R and will decrease the voltage V_R at relay location. These changes further reduces the value of Z_{seen} [13].

2.1 Distance Relay Performance During Power Swing

Due to a large disturbance such as switching of large loads, line contingencies or faults, the power flow in the transmission lines oscillates. These oscillations are known as power swings. A distance relay realizes these swings as changed in impedance and thus treat the power swing as a faulty condition [14]. The power swing phenomenon can be understood using the system shown in Fig. 1 and Eq. (1). The voltage seen by the relay V_R and the current seen by the relay I_R can be expressed by:

$$V_R = E_1\angle\delta - I_R Z_1 \text{ and } I_R = \frac{E_1\angle\delta - E_2\angle 0}{Z_T} \tag{2}$$

The value of V_R and I_R replaced in Eq. (1) and rearranging the equation for Z_{seen}:

$$Z_{seen} = \left(\frac{E_1\angle\delta}{E_1\angle\delta - E_2\angle 0} \times Z_T\right) - Z_1 = \left(\frac{1}{1 - \frac{E_2\angle -\delta}{E_1}} \times Z_T\right) - Z_1 \tag{3}$$

Here, $Z_T = Z_1 + Z_L + Z_2$ is the total impedance. Also in Eq. (3), assuming that the voltage ratio $E_2/E_1 = k$, thus:

$$Z_{seen} = \left(\frac{1}{1 - k(\cos\delta + j\sin\delta)} \times Z_T\right) - Z_1 \tag{4}$$

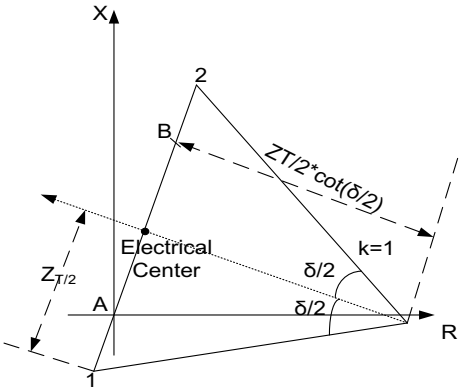

Fig. 2 Representation of Eq. (5) on R-X plane

In Eq. (4) if voltages E_1 and E_2 are equal so $k = 1$, then Eq. (4) will be modified to

$$Z_{seen} = \left(\frac{1}{1 - (\cos\delta + \mathrm{j}\,\sin\delta)} \times Z_T\right) - Z_1$$

or

$$Z_{seen} = \left(-Z_1 + \frac{Z_T}{2}\right) - j\left(j\frac{Z_T}{2}\cot\frac{\delta}{2}\right) \tag{5}$$

On the R-X plane, the Eq. (5) can be represented as shown in Fig. 2. In Eq. (5), the term $\left(-Z_1 + \frac{Z_T}{2}\right)$ represents a constant offset and $\left(j\frac{Z_T}{2}\cot\frac{\delta}{2}\right)$ represents a perpendicular line segment on the constant offset. As $k = 1$, the swing locus is a straight line that cuts the impedance line at the electrical center.

If voltages E_1 and E_2 are not equal, then Eq. (4) will be represented as:

$$Z_{seen} = -Z_1 + \frac{k[(k - \cos\delta) - j\sin\delta]}{(k - \cos\delta)^2 + (\sin\delta)^2} \times Z_T \tag{6}$$

Here, Eq. (6) represents the family of the circles with δ as a variable and k as a parameter as represented in Fig. 3. If the impedance swing remains in the distance relay characteristic, the distance relay measures it as a fault and operates.

2.2 Distance Relay Performance During Load Encroachment

During load encroachment condition, the impedance measured by a distance relay determined by the loadability limit at a specified power factor exceeds due to load voltage and current. The loadability limit is defined in VA for a distance relay at

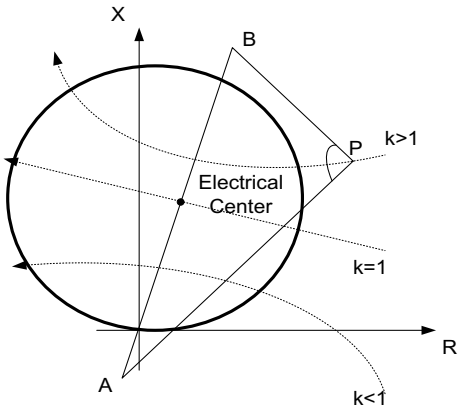

Fig. 3 MHO relay characteristic for Fig. 1

nominal voltage and a specified power factor. The load encroachment is prevalent in long heavily loaded transmission lines and in zone-III of distance relay [15]. For understanding the load encroachment phenomenon, consider the voltage of bus A in Fig. 1 is represented by V_R, the active power flow from bus A to B is P_{AB} and the reactive power flow from bus A to B is Q_{AB}. If the current flowing from bus A to B is I_R, then Eq. (7) defines the relation between P_{AB}, Q_{AB}, $V_{R,}$ and I_R.

$$P_{AB} - jQ_{AB} = V_R * I_R \tag{7}$$

The value of I_{R} from Eq. (1) is replaced in Eq. (7) we have

$$P_{AB} - jQ_{AB} = V_R * \frac{V_R}{Z_{seen}}$$

$$Z_{seen} = \frac{V_R^2(P_{AB} + jQ_{AB})}{P_{AB}^2 + Q_{AB}^2} \tag{8}$$

From Eq. (8) it is clear that the apparent power flows through the line (i.e. increase in the loading condition) is inversely proportional to the impedance seen by the relay. Due to high loading, the impedance seen by the relay may reduce and fall under the zone-III characteristic and creates unnecessary tripping.

2.3 Distance Relay Performance During Voltage Instability

From Eq. (8) it is observed that the impedance seen by the distance relay is proportional to the square of the bus voltage magnitude. Thus a reduction in voltage also decreases the impedance seen by the relay. There is a possibility for the unwanted operation of distance relay in voltage instability scenarios. In a power system, the

voltage instability conditions arise due to a reduction in voltage at several locations or the increased in reactive power of the loads connected at different locations. In a modern power system, the stressed voltage condition may occur due to other reasons that include generator reactive power limit and voltage limits, characteristic of FACTS devices, the action of tap changing transformers, voltage sensitivity of loads, etc. [16]. In such situations, the impedance seen by relay may enter into the third zone of distance relay and lead towards unnecessary tripping [17].

3 Conventional Methods to Avoid Distance Relay Mal-Operation

3.1 Distance Relay Blocking During Power Swing

The power swing is detected by measuring the change in the apparent impedance seen by the distance relay. This change is gradual during power swing compared to a faulty condition and also limited by generators inertia. For the identification of the power swing, an out-of-step (OOS) blocking unit is used. This OOS unit has a characteristic similar to the MHO relay with a larger radius. The power swing will first enter in the OOS blocking relay and then enters in the tripping relay characteristic. If the time for traveling impedance locus from OOS relay characteristic to entering tripping relay characteristic is larger than a pre-set value, the OOS relay will block the operation of distance relay [18]. The decrease in the area of third zone characteristic also reduces the chances of relay operation during power swing. The relay characteristic area can be changed with the method discussed in the next section.

3.2 Distance Relay Blocking During Load Encroachment

The distance relay operation under load encroachment is undesirable and methods discussed below are normally used to avoid this undesirable operation [19]:

- In MHO relays, the reach is maximum at an angle known as maximum torque angle. Increase in the maximum torque angle shifts the relay characteristic, decreases the load angle and increase the loadability limit of the relay [20].
- To reduce the large area of third zone of MHO relay, blinders are provided in series with the MHO relay along the R axis. As the blinders move towards the origin, the area of operation of relay reduces and loadability limit increases [20].
- The MHO relay's circular characteristic could easily be changed to a lens by adjusting the coincident timer. A lens structure has less chances of tripping during power swing due to less area on R-X plane. Also the loadability limit will increase by the using the lens structure [20].

- In a faulty condition, the voltage, current and power angles changes instantaneously, when compared to a stressed system condition. This property is utilized for OOS blocking using offset MHO relays. Fully offset MHO relays are suitable for the remote backup or for third zone protection. With the implementation of the offset backup, the loadability limit also increases [20].

3.3 Distance Relay Blocking During Stressed Voltage Conditions

For a distance relay, it is difficult to discriminate a symmetrical fault and stressed voltage condition and sometimes relay operates in its third zone due to voltage instability. During a faulty scenario, the rate of change of voltage is high compared to stressed voltage situation. Thus rate of change of voltage is considered as a discriminating element between fault and voltage instability. But the change in voltage may also takes place due to switching of capacitors, line and reactors thus these elements are needed to be considered while looking for voltage change [3]. Voltage stability indices are used to predict the voltage instability in the system. Thus, voltage stability index is also considered for discrimination in fault and voltage instability [21].

4 Proposed Method

With the advancement in PMU technology, real-time state estimation of the bulk power system is now possible. PMU provides the time-synchronized data of voltage, currents, and phase angles. Optimally located PMUs may provide the real-time power flow of a bulk power network. In the proposed method, PMUs data is utilized for calculating the real-time active and reactive powers of load buses. PMUs are the back-bone of WAMS and failure of PMUs may cause large scale blackouts. Thus the availability of PMU is an important factor while designing a WAMS.

For an illustration of the proposed method, IEEE 3 bus system is used as shown in Fig. 4. PMUs connected to buses 1 and 3 will provides the voltage and current phasors for the calculation of the real-time load active and reactive power measurement.

4.1 Understanding Scenarios for the Proposed Algorithm

4.1.1 Case-I: Normal System Condition

At rated generation and loading conditions, the system shown in Fig. 4 is simulated on MATLAB Simulink. The impedance seen by the relay R (Z_{seen}) is recorded and shown in Fig. 5a. From Fig. 5a, it is clear that Z_{seen} is constant and high (330) during

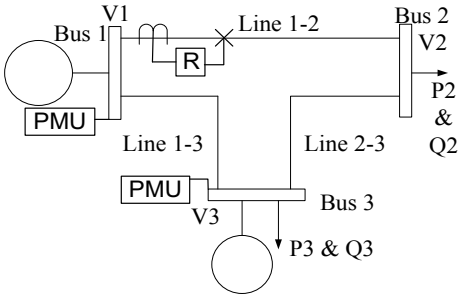

Fig. 4 IEEE-3 bus system

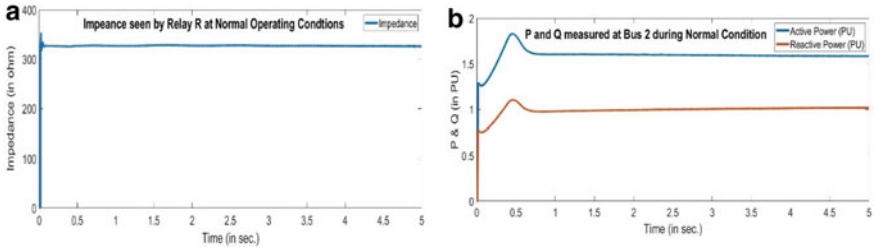

Fig. 5 **a** Measured Z_{seen} for relay R. **b** Active and reactive power at load bus 2

normal operation and it will not enter the operating zone of relay R. The active and reactive power supplied to the load at bus 2 is shown in Fig. 5b.

4.1.2 Case-II: Fault in Line 1–2 at 70% of Line Length

The system of Fig. 4 is simulated again and a three-phase fault is created in line 1–2 at 70% of line length from bus 1 at 1 s. Due to the fault, Z_{seen} is decreased to a low value as shown in Fig. 6a. This low value of impedance normally comes under the zone-I characteristic of relay R. If the relay is set to trip for such a scenario, it will

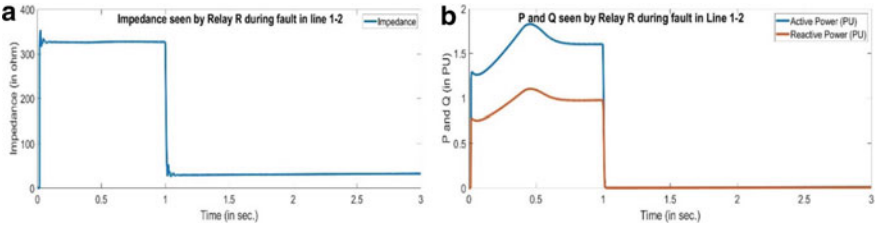

Fig. 6 **a** Measured Z_{seen} for relay R. **b** Active and reactive power at load bus 2

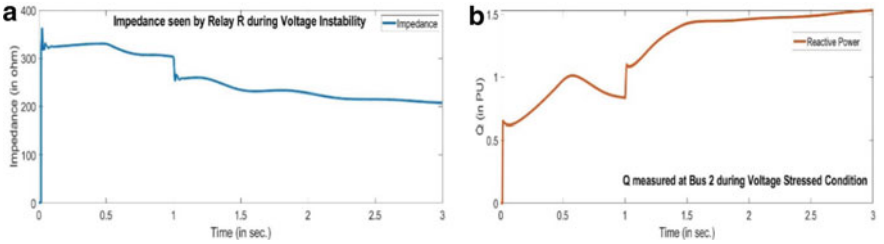

Fig. 7 **a** Measured Z_{seen} for relay R. **b** Reactive power at bus

trip in its zone-I. During this period, the active and reactive powers at the load end will also reduce as seen from Fig. 6b.

4.1.3 Case-III: Creating Voltage Instability

The voltage instability condition is created by increasing the amount of reactive power consumption at bus 2 with line 2–3 switch off. At 1 s., the reactive power of bus 2 is doubled that makes the Z_{seen} reduce from its normal value as shown in Fig. 7a. This reduced value of Z_{seen} may insert in the relay operating characteristic, especially in zone-III. During this period the active power at bus 2 remains constant. The reactive power at bus 2 as shown in Fig. 7b is increased significantly. It is visible that the impedance is reduced without any fault in the system but the measured reactive power at load end clearly reflecting a stressed system condition.

4.1.4 Case-IV: Creating Load Encroachment Condition

For this condition, the bus 2 load is increased to double of its rated value at 1 s. Figure 8a shows that the Z_{seen} is reduced from its normal value and may enter in zone-III relay characteristic. While, the increased amount of active and reactive power at bus 2 shown in Fig. 8b differentiating this scenario from the faulty condition.

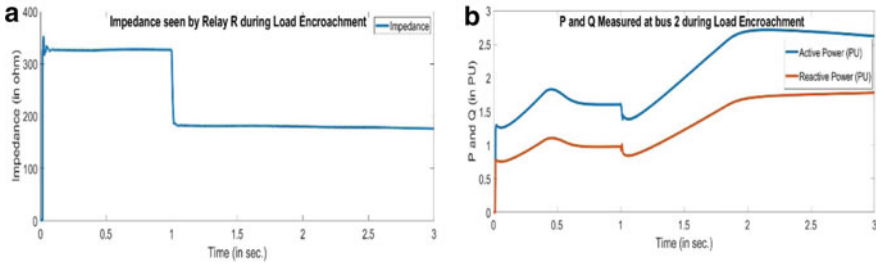

Fig. 8 **a** Measured Z_{seen} for relay. **b** Active & reactive power at bus 2

Table 1 Comparison of Z_{seen} by relay R and active & reactive powers at bus-2 during various cases

Cases	Conditions on which impedances measured	Z_{seen} (Ω)	P (PU)	Q (PU)
I	Normal operating conditions	330	1.6	1.05
II	After fault at 1 s	30	0	0
III	Creating voltage stressed condition at 1 s	210	1.6	1.6
IV	Creating load encroachment condition at 1 s	180	2.6	1.8

4.2 Comparison of the Discussed Cases

The impedances seen by relay *R* and the active & reactive powers in above simulated cases are shown in Table 1.

Following are the comparative analysis of above discussed cases.

- During normal condition (Case-I), the impedance seen by the relay is 330 Ω with the rated active and reactive power load at bus 2 and 3.
- In Case-II, before the fault in line 1–2, the value of Z_{seen} is 330 Ω and the active and reactive powers at bus-2 is at rated values. A fault at 1 s. in Case-II reduces the Z_{seen} to 30 Ω and the amount of active and reactive power flow to the load connected to bus 2 is reduced to 0 PU as shown in Table 1.
- It is visible from Fig. 7, that in Case-III, initially, the Z_{seen} is 330 Ω and the active & reactive powers for load connected to bus 2 are at their rated values. The stressed condition is created at 1 s. by increasing the reactive power of bus 2 at double of its rated value that reduces the impedance seen by relay to 210 Ω.
- In Case-IV, initially, the Z_{seen} is 330 Ω and the active and reactive powers for bus 2 are their rated values as shown in Fig. 8. After creating the load encroachment condition by increasing the active and reactive powers of bus-2 at 1 s. in Case-IV, the Z_{seen} is reduced to 180 Ω.

From the above discussed cases it is clear that a fault in the system reduces the active & reactive power flow into the system and also reduce the Z_{seen}. While in a stressed system condition the impedance seen by the relay reduces while the active and/or reactive powers flow at load buses increases. This difference in the active and reactive power flow at loads is utilized here to propose a new algorithm.

4.3 Proposed Algorithm

To avoid the chances of the unwanted distance relay operation, the algorithm of distance relay is modified using the data obtained from WAMS. In WAMS, PMUs are used to collect time-synchronized voltage, currents, and phase angles. These voltage and current signals of load buses are used for calculation of real-time active and reactive powers connected to load buses. The flow chart of the proposed method is shown in Fig. 9.

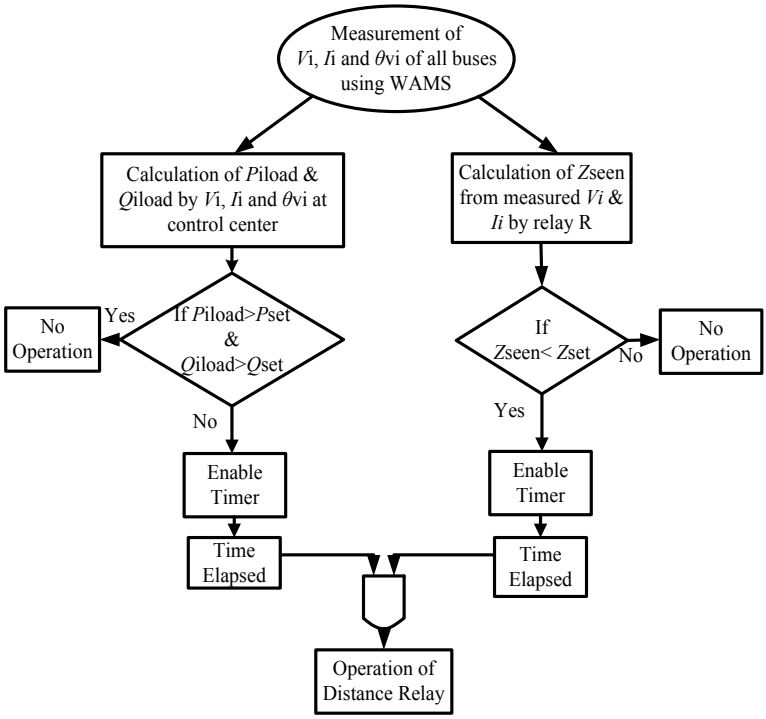

Fig. 9 Flow chart of the proposed algorithm

The first condition is the conventional condition in which if the value of impedance seen by the relay Z_{seen} is less than the set value of relay impedance Z_{set}, the relay will operate. The first condition is expressed in Eq. (9).

$$Z_{seen} < Z_{set} \tag{9}$$

The scenario of Eq. (9) may come either due to faulty condition or due to stressed system conditions discussed in Sect. 2. To avoid the operation of distance relay in stressed situations, a second operating condition is added here which is based on the parameters obtained from WAMS. The voltage and currents obtained from WAMS is used for calculation of real-time active P_{iload} and reactive power flow of load buses Q_{iload}. The load encroachment and voltage instability condition occur when the value of P_{iload} and/or Q_{iload} increased from its rated value. The power swing condition may occur in the system when there is a fault in other transmission lines or a large generator may trip. In all such conditions, the value of P_{iload} and Q_{iload} will not reduce to zero. The P_{iload} and Q_{iload} will be reduced to zero only when there is a fault in the transmission line that is supplying the load P_{iload} and Q_{iload}. Based on the logic discussed here, another condition is proposed for the operation of the distance relay. Equation (10) describe the operating condition of the distance relay. If

the value of real-time load bus active and reactive powers reduces below a set value P_{set}, the distance relay will operate.

$$P_{iload} < P_{set} \& Q_{iload} < Q_{set} \tag{10}$$

Here, P_{set} and Q_{set} are predefined settings of active & reactive power. It must be noted that distance relay will operate only when both Eqs. (9) and (10) will be satisfied.

5 Case Study

5.1 WSCC-9 Bus System

In WSCC-9 bus system shown in Fig. 10, a 3-stepped distance relay R is placed near bus 7 in line 7–8. The setting of distance relay is such that zone-I consist of 80% of the line 7–8 length, zone-II covers full length of line 7–8 and 50% of the adjoining line 8–9 and zone-III have the full length of line 8–9. The active and reactive powers at load buses is determined by using PMUs placed at optimum bus locations i.e. bus-4, bus-7 and bus-9.

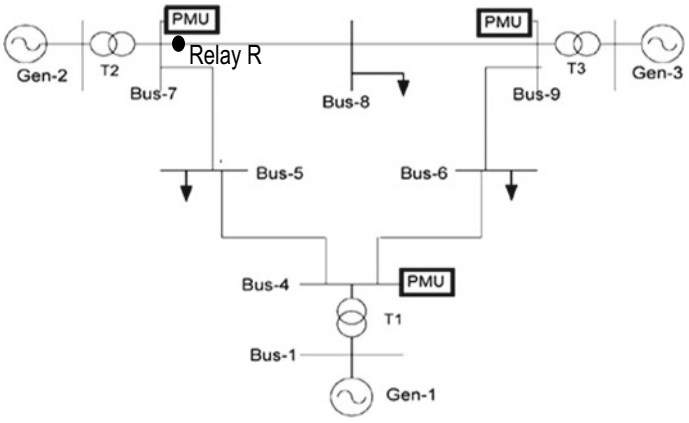

Fig. 10 WSCC-9 bus Test System

5.1.1 Calculate Active & Reactive Power of Bus-8 with Optimum PMU Location

The PMUs connected to bus 4, 7 and 9 will provide the time stamped voltage, current magnitude and phase angles of respective buses. Here, the data obtained from PMUs are utilized to calculate the real time active and reactive powers at bus 8.

Assumed that the voltage vector of bus 8 is V_8 then

$$V_8 = I_8 \times Z_{L8} \tag{11}$$

Here, I_8 is the current flowing through load 8 and Z_{L8} is the load impedance. By implementing the nodal analysis at bus 8, the current I_8 can be rewrite as:

$$I_8 = I_{78} + I_{89} \tag{12}$$

Equation (11) is modified by putting the value of I_8 from Eq. (12) as:

$$V_8 = (I_{78} + I_{89}) \times Z_{L8}$$

Here, I_{78} is the current in line 7–8, and I_{89} is the current vector of line 8–9.

$$\text{Also, } V_8 = V_7 - I_{78} \times Z_{78} \tag{13}$$

Here, V_7 is the voltage vector of the bus 7, and Z_{78} is the impedance of line 7–8. From Eqs. (12) to (13): $(I_{78} + I_{89}) \times Z_{L8} = V_7 - I_{78} \times Z_{78}$

$$\text{or } V_7 = (Z_{78} + Z_{L8}) \times I_{78} + I_{98} \times Z_{L8} \tag{14}$$

$$\text{Similarly, } V_9 = (Z_{98} + Z_{L8}) \times I_{98} + I_{78} \times Z_{L8} \tag{15}$$

On solving Eqs. (14) and (15)

$$I_{78} = \frac{V_9 Z_{L8} - V_7(Z_{89} + Z_{L8})}{Z_{L8}^2 - (Z_{L8} + Z_{78})^2} \;\&\; I_{89} = \frac{V_9 Z_{L8} - V_7(Z_{89} + Z_{L8})}{Z_{L8}^2 - (Z_{L8} + Z_{89})^2} \tag{16}$$

Putting the values of I_{78} and I_{89} from Eq. (16) and (17) to Eq. (12)

$$I_8 = \frac{Z_{89}(V_7 + V_9)}{(Z_{L8} + Z_{89})^2 - Z_{L8}^2}$$

Once the I_8 is determined from Eq. (12), V_8 can be also be determined by Eq. (11).

The value of voltage and current phasors of bus 8 i.e. V_8 and I_8 is used to determine the bus 8 active and reactive powers. These real time active and reactive powers are fed to the distance relay for implementing the proposed algorithm.

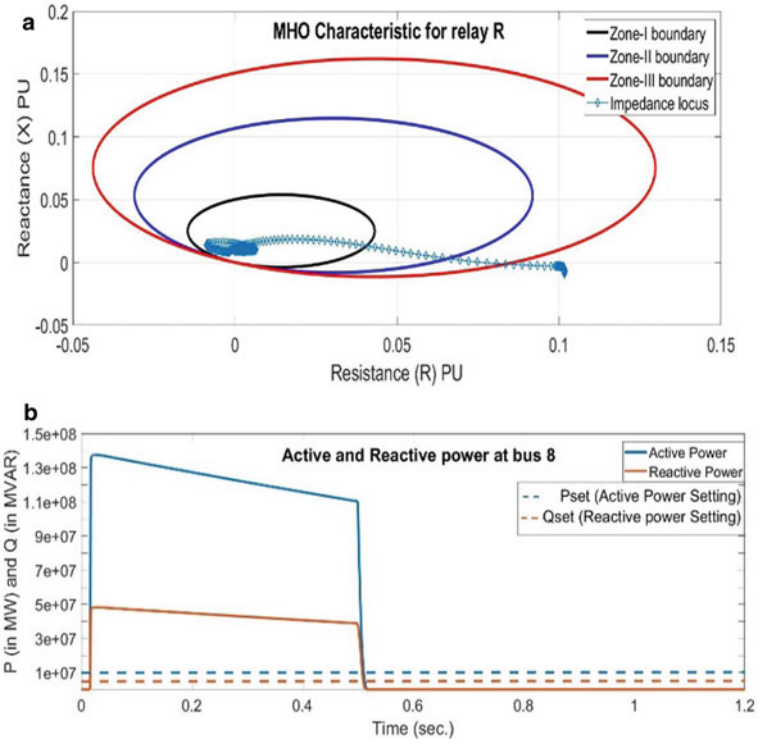

Fig. 11 **a** Relay R characteristic near bus 7 during fault condition. **b** Active and reactive power at bus 8

5.1.2 Simulated Cased on WSCC-9 Bus System

Following cases are simulated on for verification of the proposed algorithm.

Case A—During Faulty Condition Near Bus 8

In this case a fault is initiated in line 7–8 at 80% of its line length from bus-7 at 0.5 s. Figure 11a shows that due to fault, the impedance locus entered in zone-I of the distance relay. The Eq. (9) operating criteria is satisfied as the impedance locus is entering in the distance relay operating zone.

Figure 11b shows the active and reactive power of bus 8 for the simulated fault. It is clear that bus 8 active and reactive powers are reduced to zero which is below the set active power and reactive power limit i.e. P_{set} and Q_{set} respectively (10% of the rated value of bus-8).

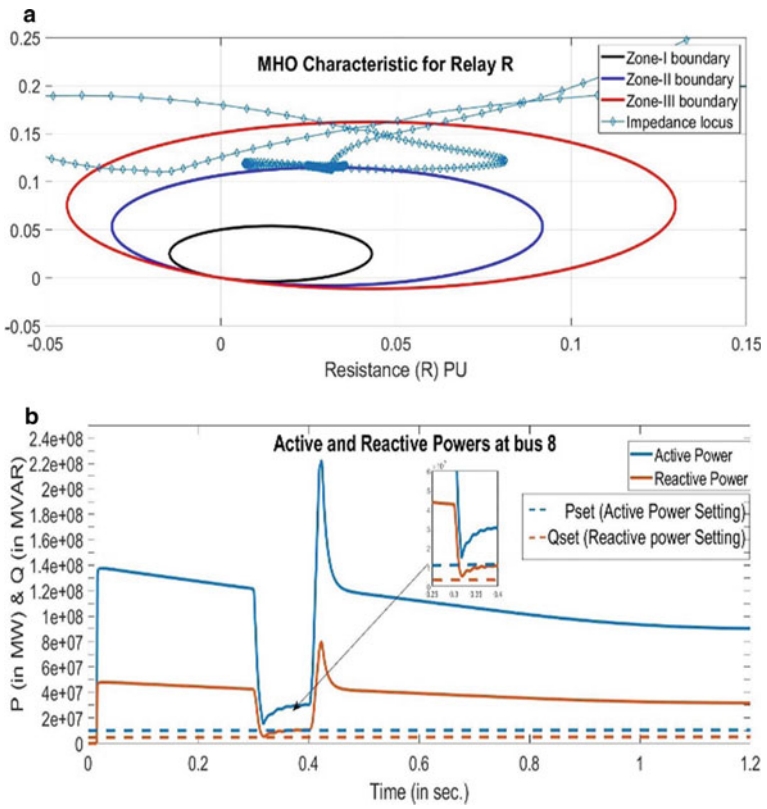

Fig. 12 **a** Relay R characteristic during power swing. **b** Active and reactive power at bus 8

The operating condition set in Eq. (10) is also confirming the operation of the relay. As both Eqs. (9) and (10) are satisfying with the given condition, the relay will operate for the simulated fault.

Case B—During Stable Power Swing at Bus 8

The stable power swing condition is initiated on line 7–8 by creating a 3-phase fault at mid-section of line 5–7 from 0.3 to 0.4 s. The fault is cleared by opening the line circuit breakers. Due to fault, the impedance locus entered in zone-III of the distance relay as shown in Fig. 12a.

Figure 12b, shows the active & reactive power flow for bus-8. It is clear that the active and reactive powers of bus-8 is not crossing the P_{set} and Q_{set} values for load bus 8. It is clear that this scenario is not satisfying the Eq. (10) operating condition. From the two of the operating condition, only one Eq. (9) is satisfying thus relay will block its operation.

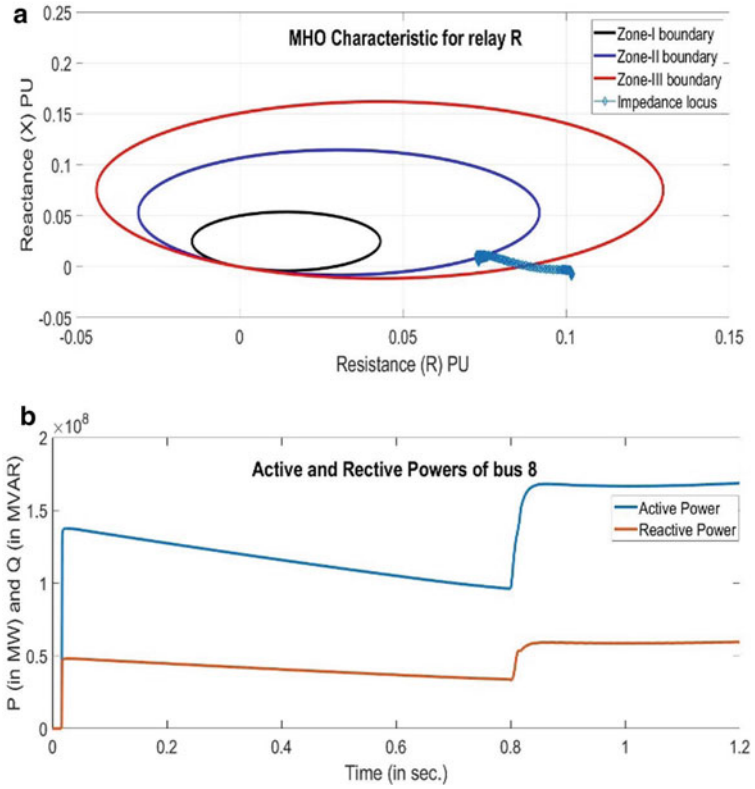

Fig. 13 **a** Relay R characteristic near bus 7 during Case-C. **b** Active and reactive power at bus-8 for Case-C

Case C—During Load Encroachment at Bus 8

For load encroachment, extreme loading condition is created at bus 8 by doubling its load as per the NERC standard of extreme loading criteria. Figure 13a shows that the relay R characteristic with impedance locus tending towards zone-III due to load encroachment condition. As the Z_{seen} reduced from the value of Z_{set}, it will operate a conventional distance relay as it satisfies the operation criteria mentioned in Eq. (9). It is clear that without any fault, the impedance is inserting in zone-III of the distance relay. However, Fig. 13b shows the active and reactive powers at bus 8. It is clear that the real and reactive power of bus 8 is higher than the set values and thus Eq. (10) is not satisfied that blocks the distance relay operation.

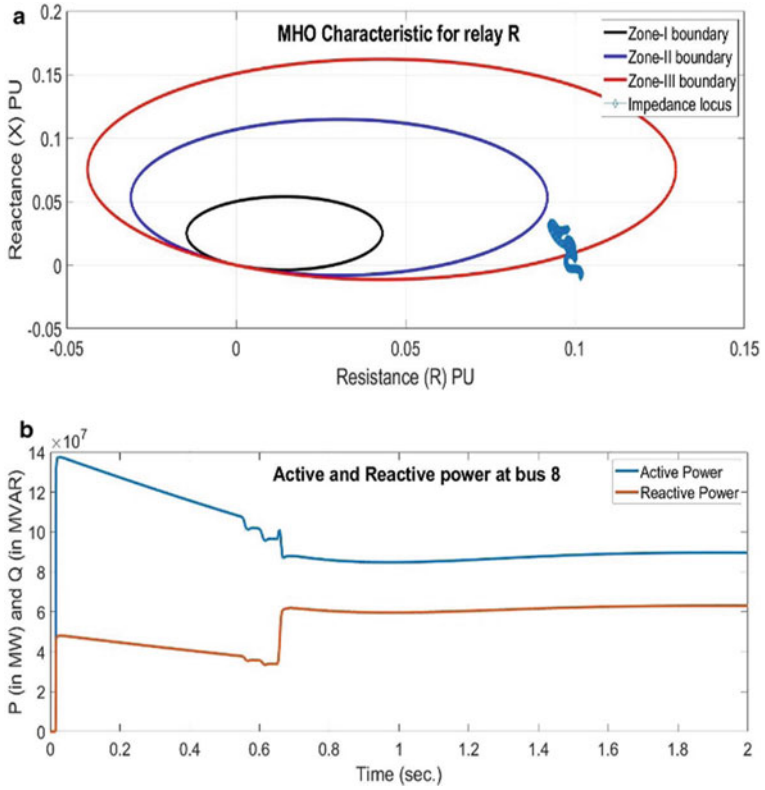

Fig. 14 **a** Relay R characteristic for Case-D. **b** Active and reactive power at bus 8

Case D—During Voltage Instability at Bus 8

The voltage instability situation is imposed by increasing the amount of reactive powers of load connected to bus 5, 6 and 8 such that the impedance locus enters in zone-III of relay R as shown in Fig. 14a. Figure 14b shows the active and reactive powers of bus 8 indicating a no-fault condition. From the power flow, it is clear the locus entering the zone-III is due to voltage instability condition and thus proposed method prevents the relay operation. The active and reactive powers of bus-8 is only shown in the Fig. 14b because the relay placed in line 7–8 will have the active and reactive power data of bus-8 for its operation.

5.2 IEEE 14 Bus System

The proposed scheme is also tested on IEEE 14- bus system shown in Fig. 15. The three stepped distance relay R_1 is placed in line 9–14 on bus 9. The settings of

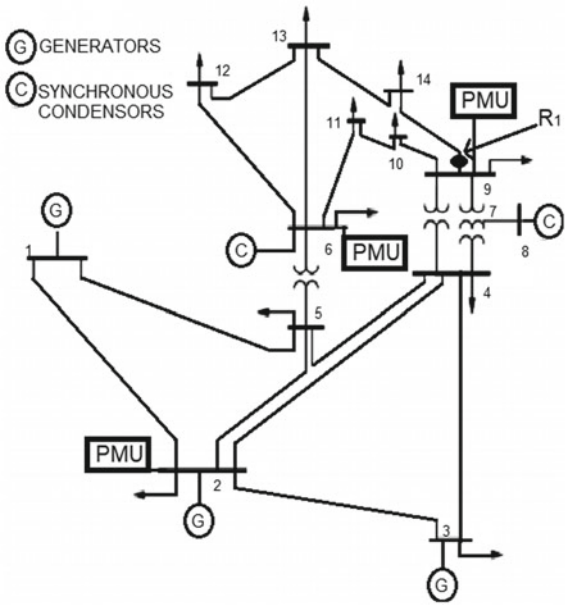

Fig. 15 IEEE 14-bus test system [22]

distance relay are such that zone-I consist of 80% of line length 9–14, the second zone includes 50% of line 14–13 and third zone covers full length of line 14–13.

The proposed scheme requires real-time active & reactive power of load bus 13.

Optimum PMU placed at bus 2, 6 and 9 will provide the load bus-8 voltage and currents as discussed in Sect. 5.1.1 for WSCC-9 bus system. The real-time load powers are fed to the relay for implementing the proposed algorithm.

5.2.1 Simulated Cased on IEEE-14 Bus System

Following cases are conducted for verification of the proposed algorithm.

Case A—During Faulty Condition in Line 13–14

Figure 16a shows that the impedance is approaching in Zone-II during the faulty condition. This condition is fulfilling the operating condition of the distance relay mentioned in Eq. (9). The second condition of the proposed approach will look towards the active power P_{13load} and reactive powers Q_{13load} of bus 13 for the relay operation. The fault is reducing the active and reactive powers of bus 13 to zero as shown in Fig. 16b. The P_{set} and Q_{set} are considered here to 10% of the rated value of load connected to bus 13. It is clear here that

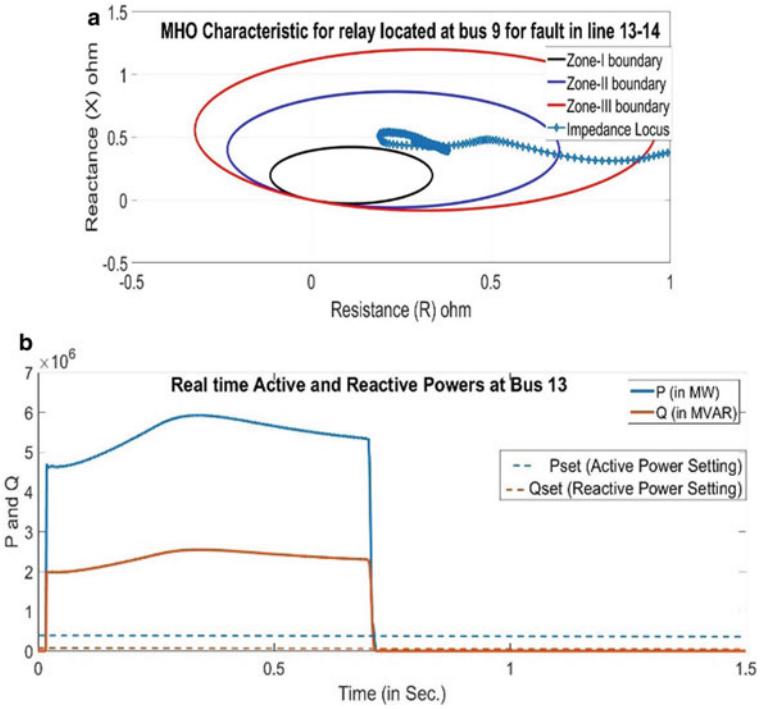

Fig. 16 **a** Relay R_1 characteristic during fault. **b** Active and reactive powers at bus 13 during fault

$$P_{13load} < P_{set}$$

$$Q_{13load} < Q_{set}$$

This scenario is satisfying the Eq. (10). As both Eqs. (9) and (10) are true for the given fault, the proposed algorithm will trip the relay.

Case B—During Stable Power Swing at Bus 13

For stable power swing, a temporary 3-phase fault is initiated on line 9–10 from 0.7 to 1.2 s. The Z_{seen} by relay placed at bus 9 observe this condition as a fault in its zone-II. The impedance trajectory is shown in Fig. 17a. It is clear that Z_{seen} is reduced and satisfies the operating condition discussed in Eq. (9). A conventional distance relay will operate in this a scenario. In the proposed algorithm, the relay will also look for active & reactive powers of bus 13 shown in Fig. 17b. It is clear that the active & reactive power of bus 13 is reducing due to fault but not going beyond the relay setting. P_{set} and Q_{set}. Due to this, the criteria for the operation of the relay shown in Eq. (10) is not fulfilled and the relay avoids the tripping.

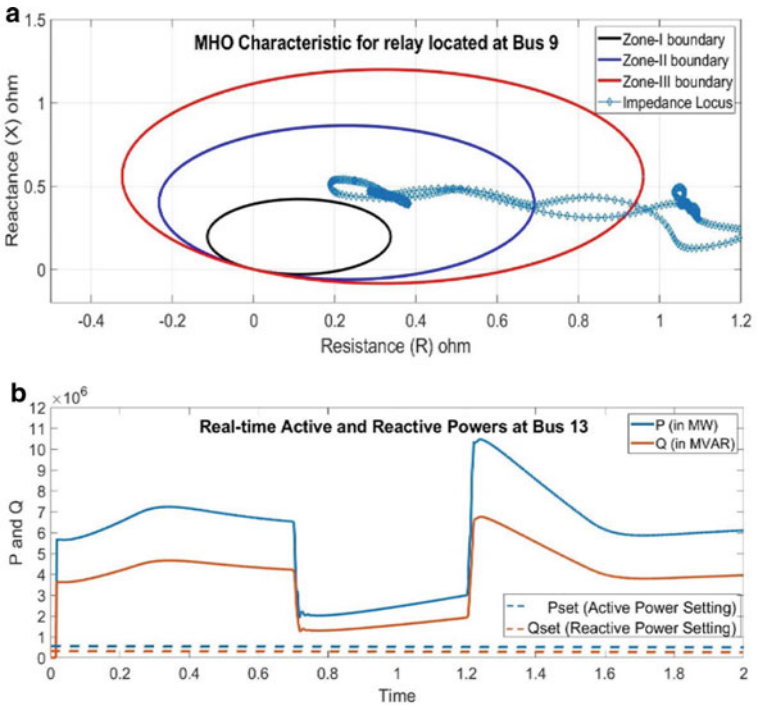

Fig. 17 **a** Relay R_1 characteristic during power swing. **b** Active & reactive powers at bus 13 during Case B

Case C—During Load Encroachment at Bus 13

For load encroachment, extreme loading condition is created at bus 13 and 14 by doubling its load as per the NERC standard of extreme loading condition. Figure 18a shows that the relay R_1 characteristic with impedance locus tending towards zone-III due to load encroachment.

As the Z_{seen} reduced, it may operate a conventional distance relay as it satisfies the operation criteria of Eq. (9). Figure 18b shows the active and reactive powers at bus 13. It is clear that the real and reactive power of bus 13 i.e. $P_{13\text{load}}$ and $Q_{13\text{load}}$ is higher than the set values P_{set} and Q_{set}. As the condition of Eq. (10) is not satisfied, the proposed algorithm avoids the operation of the distance relay.

Case D—During Voltage Instability at Bus 13

The voltage instability conditions in a power system may also operate a distance relay as the impedance trajectory enters in the zone-III of distance relay. The voltage instability the situation is created by increasing the reactive powers of bus 10, 13 and 14 such that the impedance locus enters in zone-III of relay R_1 as shown in Fig. 19a.

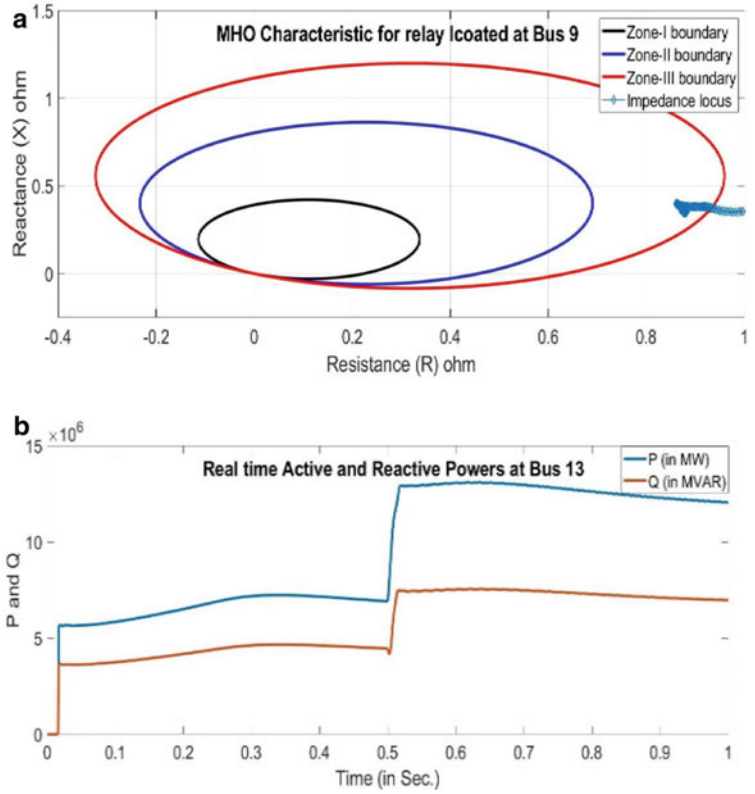

Fig. 18 **a** Relay R_1 characteristic during load encroachment. **b** Active & reactive powers at bus 13 during load encroachment

Figure 19b shows the active and reactive powers of bus 10, 13 and 14 indicating a no-fault condition. From the power flow, it is clear the locus entering the zone-III is due to voltage instability condition and thus proposed method prevents the relay operation.

5.3 IEEE 30 Bus System

Proposed scheme is also tested on IEEE 30 bus system discussed in [23]. The three stepped distance relay R_1 is placed in line 15–23 on bus 15. The settings of distance relay are such that zone-I consist of 80% of line 15–23, the second zone includes 50% of line 23–24 and third zone covers full length of line 23–24. As the system complexity increased here, real time active and reactive power of two load buses (bus 23 and 24) are fed to the relay for its operation.

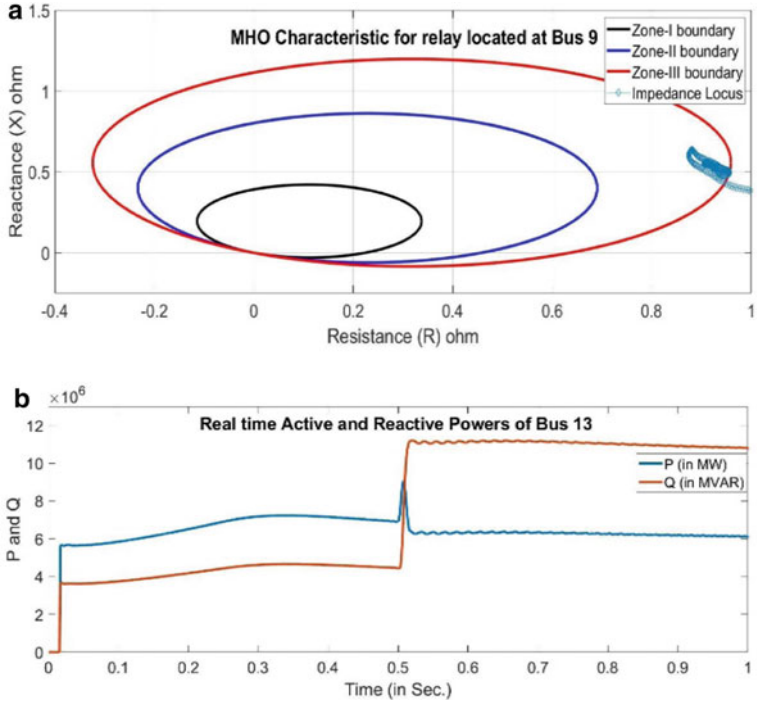

Fig. 19 **a** Relay R_1 characteristic during voltage instability. **b** Active & reactive powers during voltage instability

5.3.1 Simulated Cases on IEEE-30 Bus System

Following cases are conducted for verification of the proposed algorithm on IEEE 30 bus system.

Case A—During Normal Operating Condition

During normal operating condition, the impedance seen by the relay is high enough represented in Fig. 20a. Figure 20b shows the flow of active and reactive power in load bus 24. Figure 20 clearly shows that the relay will not operate during normal operating condition because the operating criteria set by Eqs. (9) and (10) will not be satisfied.

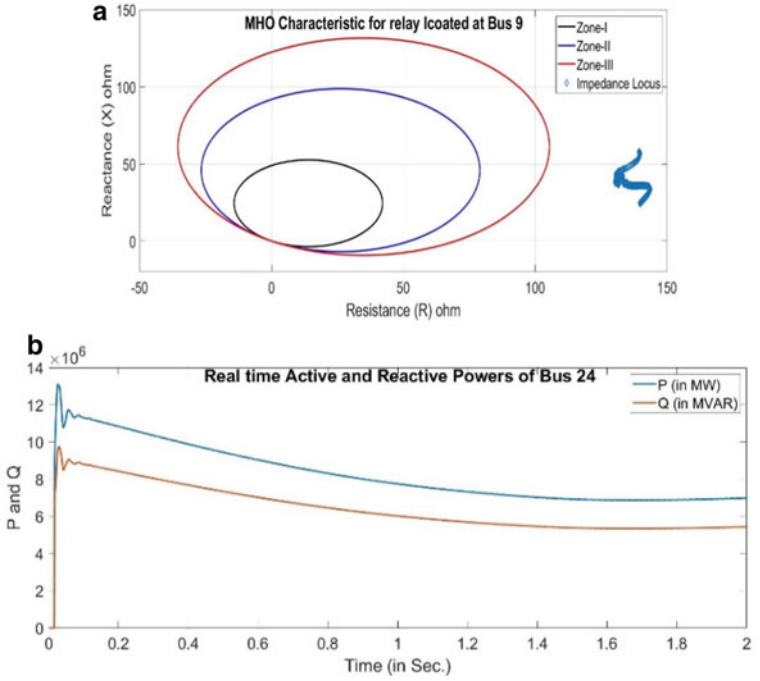

Fig. 20 **a** Relay R_1 characteristic during normal condition. **b** Active and reactive powers at Bus 24

Case B—During Fault Condition

To check the relay performance during a faulty condition, a fault is initiated in line 15–23. Figure 21a shows that the impedance is approaching in Zone-I during the faulty condition. This condition is fulfilling the operating criteria of the distance relay mentioned in Eq. (9).

The second condition of the proposed approach will look towards the active power and reactive powers of load buses for the relay operation. The fault is reducing the active and reactive powers of bus 23 to zero as shown in Fig. 21b. This scenario is satisfying the Eq. (10).

As operating criteria of both Eqs. (9) and (10) are satisfying for the given fault, the proposed algorithm will trip the relay.

Case C—During Stable Power Swing

For stable power swing, a temporary 3-phase fault is initiated on line 24-25. The Z_{seen} by relay placed at bus 15 observe this condition as a fault in its zone-III. The impedance trajectory is shown in Fig. 22a. It is clear that Z_{seen} is reduced and

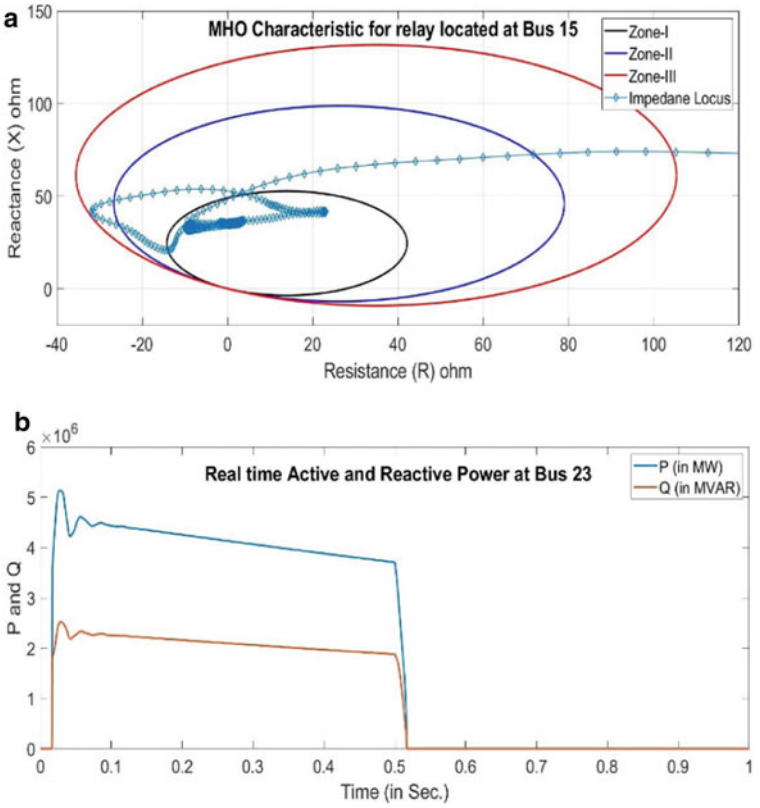

Fig. 21 **a** Relay R_1 characteristic during power swing. **b** Active & reactive powers at bus 24 during Case B

satisfies the operating condition discussed in Eq. (9). A conventional distance relay will operate in this a scenario.

In the proposed algorithm, the relay will also look for active & reactive powers of bus 23 and 24. The active and reactive powers of bus 24 is shown in Fig. 22b. It is clear from the Fig. 22b that the active and reactive powers are not reducing to zero as in previous case. A suitable value of P_{set} and Q_{set} discussed in Eq. (10) may block the unwanted operation of distance relay.

Case D—During Load Encroachment

For load encroachment, extreme loading condition is created at bus 23 and 24 by doubling its load. Figure 23a shows that the relay R_1 characteristic with impedance locus tending towards zone-III due to load encroachment. As the Z_{seen} reduced, it may operate a conventional distance relay as it satisfies the operation criteria of Eq. (9).

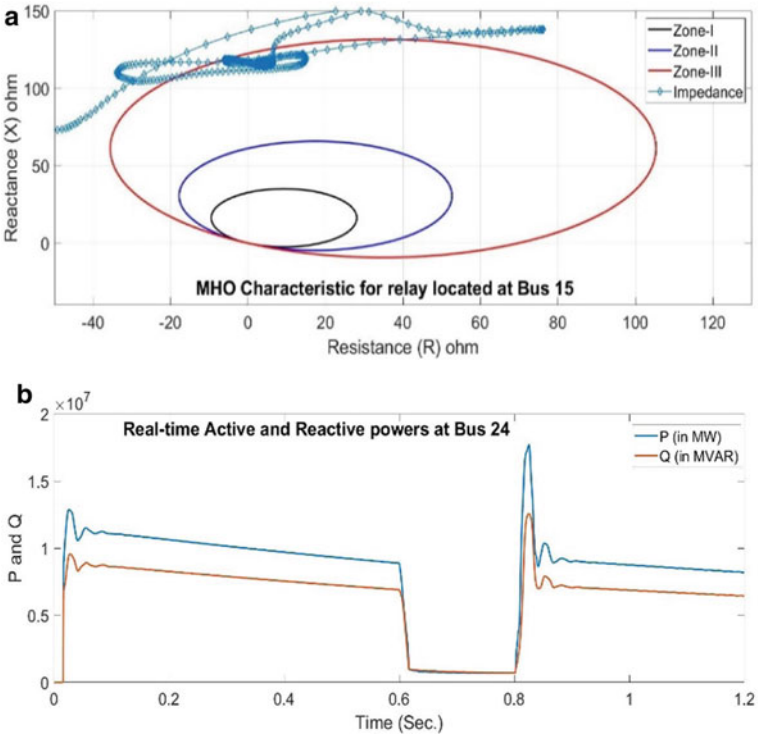

Fig. 22 **a** Relay R_1 characteristic during power swing. **b** Active & reactive powers at bus 24 during Case B

Figure 23b shows the active and reactive powers at bus 24. It is clear that the real and reactive power of bus 24 is higher than the rated values. It is not satisfying the operating criteria discussed in Eq. (10). The proposed algorithm avoids the operation of the distance relay.

5.4 Comparison with Existing Methods

The proposed algorithm is tested on the WSCC-9, IEEE-14 and IEEE-30 bus test systems for various cases such as stable load encroachment, power swing, and voltage instability condition. It is found that the active & reactive power at load buses have significant difference during faults and abnormal operating conditions. The load bus powers are utilized for blocking the relay operation with the proposed algorithm. The proposed method is compared with the existing methods discussed in literature based on the following points:

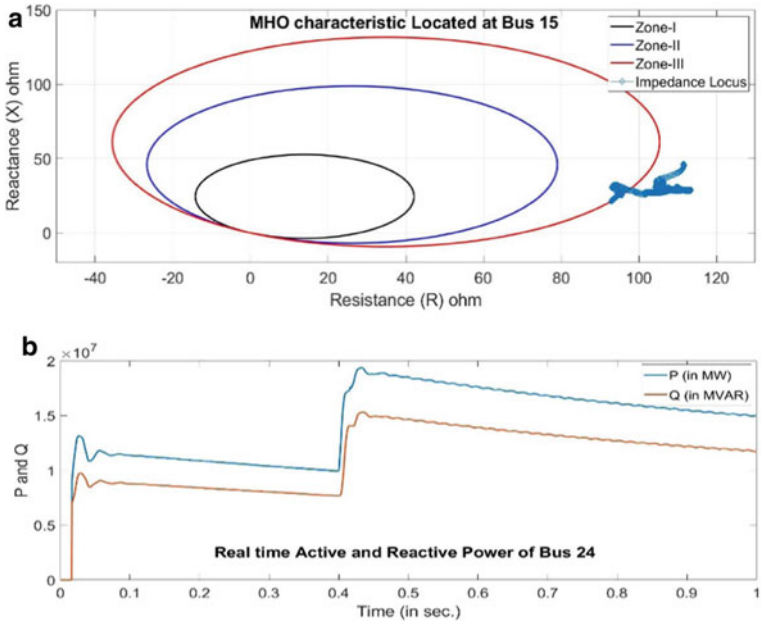

Fig. 23 **a** Relay R_1 characteristic during load encroachment. **b** Active & reactive powers during load encroachment

1. PMUs Location: The methods represented in [7–9, 12] need the PMU at all buses of a network. For practical applications, PMUs are placed only at optimal locations for the data collection. The proposed method does not require the PMU at all locations and utilizes the optimal PMU data for decision making. This also makes the approach more economical in practical perspective.
2. Training Requirement: The methods discussed in [5, 6, 12] needs to train the model before implementation. This training process can be done offline but needs large data sets for effective results. While the proposed method does not require any data training model.
3. Network conversion: The method discussed in [8, 10] required to convert the complete network in an equivalent TE model or SMIB system. The conversion of a real-time network into another equivalent model needs additional computational time. In the proposed method, there is no need to convert the network into another equivalent network, thus reduces the computational burden.
4. Utilization of wide-area information: Protection scheme discussed in [5, 6] makes the operating decision based on the local information. In a large system decision making using only the local information may lead to unwanted relay operation. The proposed method utilizes the WAMS and has high accuracy in the prediction of the power system state.

Table 2 Comparison of different methods

Methods→	[5]	[6]	[7]	[8]	[9]	[10]	[12]	Proposed
PMUs Locations	–	–	All	All	All	Optimum	All	Optimum
Training required	✓	✓	✓	✘	✘	✘	✓	✘
Network Conversion	✘	✘	✘	✓	✘	✓	✘	✘
Wide area information	✘	✘	✓	✓	✓	✓	✓	✓
Applicable for Load Encroachment	✘	✘	✓	✓	✓	✓	✘	✓

Table 2 represents a comparison of the proposed method with the existing methods. The Load encroachment phenomenon which is not considered by few authors is also incorporated in the existing method to avoid distance relay mal-operation.

6 Conclusion

Advancement in the WAMS technology opens the door for researchers to propose new algorithms for power system operation, control, and protection. The protection schemes implemented using WAMS reduces the risks of large area blackouts. Unwanted distance relay mal-operation may create cascaded system tripping and it is one of the reasons for large area blackouts. This chapter utilizes the data from WAMS to address the issues of unwanted distance relay operation due to stressed system conditions. The scenarios in which a distance relay mal-operates are thoroughly discussed in this work. Based on the observations from the simulation on IEEE 3 bus system, a method has been proposed to avoid the unwanted operation of distance relay using monitored changes in load active and reactive power. Real-time current and voltage phasors obtained from optimally located PMUs are utilized for calculation of load active and reactive power. To check the effectiveness of the proposed algorithm, various cases are simulated on WSCC-9 bus, IEEE-14 bus and IEEE-30 bus test systems. It is observed that the proposed method successfully blocks the distance relay operation under stressed system conditions.

References

1. G. Benmouyal, D. Hou, D. Tziouvatas, Zero-setting power-swing blocking protection, in *31st Annual Western Protective Relay Conference* (WA, USA, 2004)
2. X. Lin, Y. Gao, P. Liu, A novel scheme to identify symmetrical faults occurring during power swings. IEEE Trans. Power Deliv. **23**, 73–78 (2008)
3. M. Jonsson, J. Daalder, An adaptive scheme to prevent undesirable distance protection operation during voltage instability. IEEE Trans. Power Deliv. **18**(4), 1174–1180 (2003)

4. M. Sharifzadeh, H. Lesani, M. Sanaye-Pasand, A new algorithm to stabilize distance relay operation during voltage degraded conditions. IEEE Trans. Power Deliv. **29**(4), 1639–1647 (2014)
5. K. Seethalekshmi, S. Singh, S. Srivastava, A classification approach using support vector machines to prevent distance relay maloperation under power swing and voltage instability. IEEE Trans. Power Deliv. **27**(3), 1124–1133 (2012)
6. A. Swetapadma, A. Yadav, Data mining based fault during power swing identification in power transmission system. IET Sci. Meas. Technol. **10**(2), 130–139 (2016)
7. D. Pal, B. Mallikarjunna, R. Reddy, Synchrophasor assisted adaptive relaying methodology to prevent zone-3 mal-operation during load encroachment. IEEE Sens. J. **17**(23), 7713–7722 (2017)
8. P. Kundu, A.K. Pradhan, Enhanced protection security using the system integrity protection scheme (SIPS). IEEE Trans. Power Deliv. **31**(1), 228–235 (2016)
9. P. Gawande, S. Dambhare, New predictive analytic aised response based system integrity protection scheme. IET Gener. Transm. Distrib. **13**(8), 1204–1211 (2019)
10. S.S. Samantaray, A. Sharma, Supervising zone-3 operation of the distance relay using synchronised phasor measurements. IET Gener. Transm. Distrib. **13**(8), 1238–1246 (2018)
11. D. Kumar, J. Savier, Synchrophasor based system integrity protection scheme for an ultra-mega-power project in India. IET Gener. Transm. Distrib. **13**(8), 1220–1228 (2019)
12. S. Das, R. Dubey, B. Panigrahi, S. Samantaray, Secured zone-3 protection during power swing and voltage instability: an online approach. IET Gener. Transm. Distrib. **11**(2), 437–446 (2016)
13. Network Protection & Automation Guide, Alstom Grid (2011)
14. J. Khodaparast, M. Khederzadeh, *Adaptive Concentric Power Swing Blocker. Protection and Control of Modern Power Systems*, vol. 1, no. 16 (Springer, 2016)
15. Line Protection Relay User Manual Version 3.3, ERL Phase Power Technologies (2003)
16. P. Kundur, *Power System Stability and Control* (Mc-Graw-Hill, New York, 1994)
17. R. Sodhi, S. Shrivastav, S. Singh, A simple scheme for wide area detection of impeding voltage instability. IEEE Trans. Smart Grid **3**(2), 818–827 (2012)
18. Power swing and out-of-step considerations on transmission lines, in *D6*, *IEEE Power System Relay Committee Working Group* (IEEE, 2005)
19. Increase line loadability by enabling load encroachment functions of digital relays, in *NERC Planning Committee* (New Jersey, 2005)
20. Methods to increase line relay loadability, in *NERC Planning Commission* (New Jersey, 2006)
21. H. Song, B. Lee V. Ajarappu, Control strategies against voltage collapse considering undesired relay operations, in *Proceeding of the Institute Engineering Technology Generation Transmission and Distribution,* vol. 3, no. 2, pp. 164–172 (2009)
22. N. Rajalwal, P. Mishra, Impact of DFIG on voltage stability of a network in smart grid: an analysis, in *Technologies for Smart City Energy Security and Power*, India, 2018
23. PSCAD, IEEE-30 Bus System, (Manitoba Hydro International Ltd., Manitoba, Canada, 2018)